Abdelkader H. BOUZIANE[1], Mohammed B. DEBBAT[2], Ahmed TAHOUR[3]

LSTE Laboratory, University Mustapha Stambouli of Mascara (1), Department of Electrical Engineering, University Mustapha Stambouli of
School of Applied Sciences Tlemcen (3), Mascara, Algeria (2)

An Adaptive FLC-GAFOPI Controller for WRSG Based Wind Turbine

Abstract. This paper deals with design of an adaptive fuzzy logic control-genetic algorithm fractional order-proportional and integral (AFLC-GAFOPI) for a wound rotor synchronous generator (WRSG), based on a variable speed wind energy conversion system (WECS), for improving its power output quality . The AFLC-GAFOPI represents a hybridization of two GAFOPI and AFLC controllers respectively. The first one is designed to upgrade the performance of the system . The second one is chosen to overcome the nonlinearity of the system. To demonstrate the efficiency of the AFLC-GAFOPI controller, a comparison with the GAFOPI controller was performed for different wind regimes. The outcomes clearly demonstrate that the designed controller outperforms the compared controller in terms of response, robustness and overshoot

*Streszczenie. W artykule zajęto się projektowaniem adaptacyjnego algorytmu sterowania rozmytego, opartego na systemie konwersji energii wiatru o zmiennej prędkości (WECS). jego jakość wyjściowa mocy. AFLC-GAFOPI reprezentuje hybrydyzację odpowiednio dwóch sterowników GAFOPI i AFLC. Pierwsza ma na celu podniesienie wydajności systemu. Drugi wybierany jest w celu przezwyciężenia nieliniowości systemu. Aby zademonstrować wydajność sterownika AFLC-GAFOPI, przeprowadzono porównanie ze sterownikiem GAFOPI dla różnych warunków wiatrowych. Wyniki jasno pokazują, że zaprojektowany sterownik przewyższa porównywany sterownik pod względem odpowiedzi, niezawodności i przeregulowania. (**Adaptacyjny sterownik FLC-GAFOPI dla turbiny wiatrowej opartej na WRSG**)*

Keywords: Adaptive Fuzzy logic, fractional order, wind energy conversion system, wound rotor synchronous generator
Słowa kluczowe: sterownik adaptacyjny, logika rozmyta, turbina wiatrowa

Introduction

Considered as clean energy, wind is today a renewable energy resource and a growing sector arousing particular interest in the context of the creation of a healthy environment and a sustainable development. Since it is mainly influenced by environmental factors, it is essential to design systems that can generate maximum power under all working situations [1, 2]. A major portion of the existing wind farm (WF) is made up of grid-connected devices. There are two types of wind turbines currently on the market: fixed speed wind turbines that are connected directly to the network via the stator and variable speed wind turbines that are connected via power electronic converters. With the potential to increase performance at all wind speeds, the second category improves energy yield, minimizes mechanical loads, and enhances the electrical power quality generated. As a result, WRSG vector control with variable speed control is necessary [3].

In WECS, a variety of electric generators have been employed. The wound rotor synchronous generators (WRSG) are self-excited generators widely used in power generation systems due to their advantages including being suitable for high power generation, improved power factor as well independent control of real and reactive power assets, and having a high yield [4].

Many control systems have been investigated for controlling a WECS, with the PI controller being the most extensively utilized [5]. In recent years, studies have shown that fractional order PID controllers outperform traditional controllers. Since real engineering systems are subject to external disturbances and measurement noise therefore robustness has become essential in the design of control systems [6]. Fractional Order dynamic systems, are one of the resilient controllers used to address these difficulties [7, 8]. The FOPID controller, which has been extensively studied, has proven its efficiency and versatility, allowing for a more precise response with superior dynamics [9, 10]. Although, it should be noted that FO controllers are model dependent and only work better when a precise mathematical model is known. From the literature, fuzzy logic gives a good controlling influence for non-linear system. On the other hand, using fuzzy control only to reduce the steady-state error is a failure and the control precision is low [11]. For the control of wind turbine (WT), a

fuzzy adaptive PI controller has been proposed, in which the fuzzy controller's domain can be adaptively updated to provide excellent static performance, while speed variation cannot be well reduced [12]. In addition, a large number of parameter controllers make selecting the best gains difficult. many heuristics intelligent optimization algorithms have been applied including GA algorithm [13]. To address the aforementioned inconveniences and overcome the problems given by the non-linearity and complexity of the system, the controllers GAFOPI and FLC can be combined to provide optimal system performance [14].

This paper deals with the design of AFLC-GAFOPI controller using a fuzzy rules-based method associated with a FOPI controller where the gains of the latter are identified quickly and optimally using a genetic algorithm (GA). This type of control, called adaptive, provides better gains by fine-tuning the parameters and improves the performance of wind energy conversion during load variation and under fluctuating wind conditions. The rest of the paper is structured as follows. The modelling of the wind energy system, containing WRSG's is explained in section 2. In order to control WRSG, MPPT technique and field-oriented control are developed in section 3. The AFLC-GAFOPI controllers are designed for a machine Side Converter (MSC) and a Grid Side Converter (GSC) in section 4 and 5 respectively. Section 6 contains the simulation and comments of AFLC-GAFOPI controllers compared to that of GAFOPI controllers. The conclusion is covered in the final part.

2. Modelling of the wind energy system

As can be observed in Fig. 1, the studied system WECS is made up of a wind turbine, a gearbox, and the WRSG, which stator is linked to the grid via a back-to-back converter consisting of an (MSC) and a (GSC) through a DC bus where the latter is also linked to a DC/DC converter at the rotor winding of the WRSG. The AC/DC converter ensures the control of the generated power by acting on the generator speed with the MPPT. The DC/AC converter allows with an adequate command, to regulate the reactive power flow, the DC link voltage, and the power factor while wind fluctuations, the third converter is an excitation circuit. The action of all converters is governed by the concept of wide pulse modulation (PWM) [15].
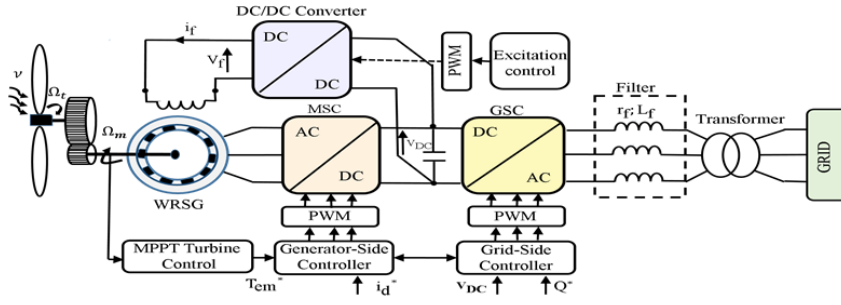
Fig.1. Wind energy conversion system based on WRSG.

2.1. Wind turbine aerodynamic mode

Wind energy is converted into mechanical energy by the wind turbine, which is stated as [16]:

(1) $$P_a = 0.5\rho\pi R^2 C_p(\lambda,\beta)v^3$$

where, ρ is the air density (kg/m3), R is the blade radius (m), v is the wind speed in (m/s). C_p is the power coefficient, which depends on at the same time the blade pitch β in (degrees) and The Tip-Speed Ratio (TSR) λ where the latter's formula is as follows

(2) $$\lambda = \frac{R\Omega_t}{v}$$

The $C_p(\lambda,\beta)$ characteristic property is depicted in Fig. 2 and is specified by [17].

(3) $$\begin{cases} C_p(\lambda,\beta) = 0.5176\left(\frac{116}{\lambda_i} - 0.4\beta - 5\right)e^{\frac{-21}{\lambda_i}} - 0.0068\lambda \\ \frac{1}{\lambda_i} = \frac{1}{\lambda + 0.08\beta} - \frac{0.035}{\beta^3 + 1} \end{cases}$$

The maximum, $C_{P\max}$ is obtained for λ_i =8.1 and for $\beta = 0°$. Therefore, there is a particular λ at which turbine system follows the $C_{P\max}$ to capture the maximum power up to the nominal speed. The mechanical equation of the generator speed is stated as

(4) $$J\frac{d\Omega_t}{dt} = T_m - T_{em} - F\Omega_m$$

where J denote the moment of inertia, F denote the viscous friction coefficient and T_m is the gearbox torque.
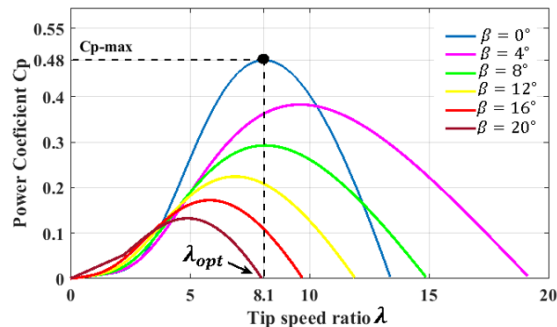
Fig. 2. Power Coefficient Compared with Tip Speed Ratio

2.2. WRSG Model

By using Park's transformation in rotating frame of reference d-q, the voltages can be defined by Eq. (5) and Eq. (6) as follows [18]:

(5) $$\begin{cases} v_{ds} = -r_s i_{ds} + \omega_e L_q i_{qs} - \omega_e M_{sQ} i_Q - L_d \frac{di_{ds}}{dt} \\ \qquad + M_{sf}\frac{di_f}{dt} + M_{sD}\frac{di_D}{dt} \\ v_{qs} = -r_s i_{qs} - \omega_e L_d i_{ds} + \omega_e M_{sf} i_f + \omega_e M_{sD} i_D \\ \qquad - L_q\frac{di_{qs}}{dt} + M_{sQ}\frac{di_Q}{dt} \end{cases}$$

(6) $$\begin{cases} v_f = r_f i_f + L_f\frac{di_f}{dt} - M_{sf}\frac{di_{ds}}{dt} + M_{fD}\frac{di_D}{dt} \\ 0 = r_D i_D + M_{fD}\frac{di_f}{dt} - M_{sD}\frac{di_{ds}}{dt} + L_D\frac{di_D}{dt} \\ 0 = r_Q i_Q - M_{sQ}\frac{di_q}{dt} + L_Q\frac{di_Q}{dt} \end{cases}$$

$v_{ds}, v_{qs}, i_{ds}, i_{qs}$ denote the stator voltages and current in the d and q axis, respectively, L_d, L_q represent the inductance od the d-axis stator winding direct and q-axis stator winding, L_D, L_Q denote the inductance of the direct and quadrature damper windings, M_{sf} is mutual inductance between the field winding and d-axis stator winding, M_{fD} is mutual inductance between the field winding and d-axis dampers winding, M_{sQ} is mutual inductance berween q-axis stator windings and q-axis damper winding, M_{sD} is mutual inductance between the d-axis stator windings and d-axis damper winding, v_f, i_f denote the main field excitation voltage and main field current, respectively, i_D, i_Q denote the direct and transverse dampers currents. The electrical rotating speed ω_Θ and the generator torque T_{em} are determined by Eq. (7) and Eq. (8)

(7) $$\omega_e = p\Omega_m ;$$

(8) $$T_{em} = p(\phi_{ds}i_{qs} - \phi_{qs}i_{ds}) = p$$
$$\left[(L_q - L_d)i_{ds}i_{qs} + (M_{sf}i_f + M_{sD}i_D)i_{qs} - M_{sQ}i_Q i_{ds}\right]$$

3. Control of the WRGS
3.1. MPPT control

The MPPT controller's goal is to produce a reference speed command that allows the WF to extract as much power as possible for a set wind speed. As a result, when the wind speed varies, the WRSG's speed is controlled to pursue the maximum power point path , and the optimal rotational speed of the WT generator Is expresssed as [19]

$$(9) \qquad \Omega_{t\_ref} = \frac{\lambda_{opt} v}{R}$$

3.2. Filed oriented control

By using the field-oriented control for the torque control, the stator current component of the d-axis $(i_{ds} = 0)$ for minimizing the generator current. Hence, we can obtain the electromagnetic torque such as [20]:

$$(10) \qquad T_{em} = p i_{qs} (M_{sf} i_f + M_{sD} i_D)$$

The reference signal is obtained as follows from Eq. (10)

$$(11) \qquad i_{qs} - ref = \frac{T_{em} - ref}{p(M_{sf} i_f + M_{sD} i_D)}$$

Using the equation Eq. (5), the decoupled control approach for d and q current loops becomes:

$$(12) \quad \begin{cases} v_{ds} = -(r_s i_{ds} + L_d \dfrac{di_{ds}}{dt}) + \omega_e L_q i_{qs} - \omega_e M_{sQ} i_Q \\ v_{qs} = -(r_s i_{qs} + L_q \dfrac{di_{qs}}{dt}) - \omega_e L_d i_{ds} + \omega_e M_{sf} i_f \\ \qquad\qquad + \omega_e M_{sD} i_D \end{cases}$$

4. Design of AFLC-GAFOPI controler

As illustrated in Fig. 3, the current control scheme used on the MSC side includes both AFLC-GAFOPI controllers which will then be compared to those of GAFOPI to verify the effectiveness of each.

4.1. Genetic Algorithm Tuned Fractional Order Controller

A fundamental topic in advanced control systems theory is in the presence of uncertainty. The control system also needs to be steady and have high transient performance. As a result, controllers that use optimized fractional order derivatives and integrals could attain these objectives while also ensuring greater
Robustness [21[.

4.1.1. FOPI controller

In the literature, fractional calculus controllers have been widely employed. The FOPI controller is a development of the standard PI controller using fractional calculus whose mathematical representation in the time domain is reported as follows [22]:

$$(13) \quad u(t) = k_p e(t) + k_i D_y^{-\lambda} e(t)$$

where u(t) denote the control signal and e(t) denote the error, k_p and k_i represent proportional and integrator

gainrespectively, λ denote the fractional integrator. The frequency domain descriptor of the FOPI is given by

$$(14) \qquad FOPI = k_p + \frac{k_i}{s^\lambda}$$

Fig.3. Bloc diagram of machine side converter controller

4.1.2. Genetic Algorithm

The GA algorithm is applied to determine the optimal parameters of k_p, k_i and λ gains. Initially, a random population of genes is chosen in the search area, and each iteration incur breeding, crossover, and mutation to give individuals and upgrade fitness (lower f value) in the following iteration [23]. In order to design a best FOPI controller, the closed loop response of the fractional order control system was developed in the Matlab environment using the integral performance criteria as it is clarified in Fig. 4 Where k_{pwm} represents gain of the power converter, T_s represents a switching period.

Fig. 4. Scheme of GAFOPI for WRSG current control

The integral time multiplied absolute Error (ITAE) criterion is used to lower the error values, and its function:

$$(15) \qquad f_i(IATE) = \int_0^\infty t \, |e(t)| dt$$

Due to its high strong selectivity, the ITAE criterion has been chosen as the algorithm's optimization index. Changes in the system parameters can significantly alter the ITAE value [24]. The parameters of the FOPI controllers are optimized within typical ranges as follows:

PI controller $f_i(k_p, k_i, \lambda)$ $\begin{cases} k_p^{min} < k_p < k_p^{max} \\ k_i^{min} < k_p < k_i^{max} \\ \lambda^{min} < \lambda < \lambda^{max} \end{cases}$

where f_i is the fitness function given by EEq. 15 and $k_x^{\min}, k_x^{\mathrm{miax}}$ denote the minimum and maximum limits of the controller gains parameters.

4.2. Adaptive fuzzy logic controller GAFOPI

Fuzzy logic theory provides additional flexibility, efficacy, and performance when tuning controller settings in system design, especially when there is a non-linear dynamic. However, there is still the risk of having low amplitude oscillations in steady state, also for the work of the FO controller, the results are not at the expected level for a nonlinear and complex system. Hence, to remedy the drawback of GAFOPI and FLC controllers, we combine both controllers. The AFLC-GAFOPI is a controller that improves the robustness of the system by combining rule- based fuzzy control with the GAFOPI controllers. The fuzzy system's adaptive technique will increase the dynamic performance of the FO controller, allowing the controller to react fast to parameter changes [14, 25]. In the suggested control structure illustrated in Fig. 5, the FLC utilizes the error and derived error input as follows:

(16)
$$\begin{cases} E(t) = e(t) \times k_e \\ \Delta E(t) = \left(e(t) \times k_e\right) - \left(e(t-1) \times k_{\Delta e}\right) \end{cases}$$

where the both input values normalized using the normalization gains $k_e, k_{\Delta e}$ and the output is a fuzzy signal $u(t)$ that permits two normalization gains G_p and G_i to be added to each FOPI gain to form a new control signal $Y(t)$ as shown by Eq. 17

(17)
$$Y(s) = \left(k_{pdqs}E(s) + G_p U(s)\right)$$
$$+ \left(k_{idqs}E(s) + G_i U(s) \frac{1}{s^\lambda}\right)$$
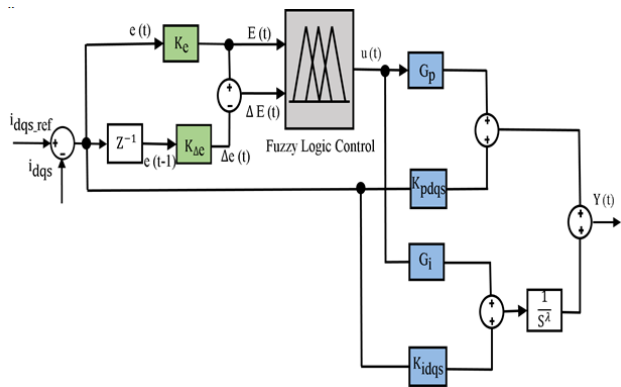
Fig. 5. Adaptive Fuzzy Logic Controller-GAFOPI structure
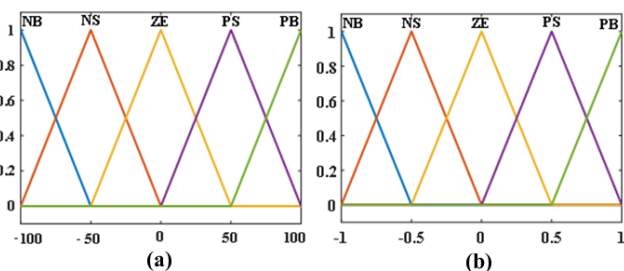
Fig. 6. (a)- Membership functions of *E and* ΔE (b)- Membership functions of *U*

As illustrated in Fig. 6, we employed triangular membership functions for the input and output variables. The fuzzy rules that give these control actions are are shown in Table 1.

Table 1. Fuzzy rules of ALFC-GAFOP

U		ΔE				
		NB	NS	ZE	PS	PB
E	NB	ZE	ZE	PB	PB	PB
	NS	ZE	ZE	PS	PS	PS
	ZE	PS	ZE	ZE	ZE	NS
	PS	NS	NS	NS	ZE	ZE
	PB	NB	NB	NB	ZE	ZE

5. Control og grid side converter

In Fig. 7 shows the intermediate circuit voltage and current controls for the GSC. Furthermore, to achieve synchronization with the electric network, the phase lock loop (PLL) method is also used.
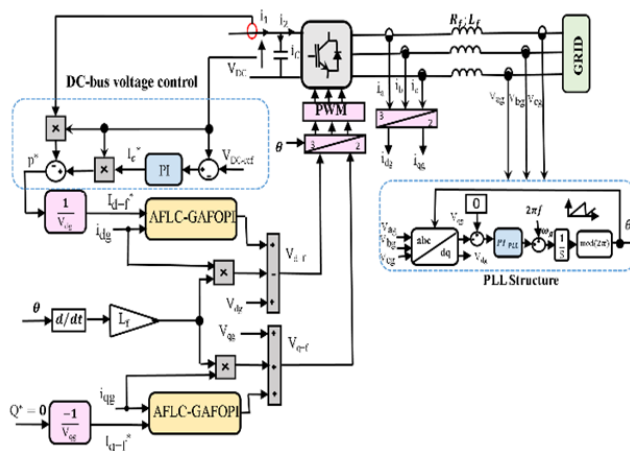
Fig. 7. Grid side converter control

5.1. Control of currents flowing through the RL filter

In this session, we choose the vector control strategy such that voltage-oriented d-q reference frame, with positive currents come from the converter to the grid, so that its quadrature component $(V_{qg} = 0)$ and $(V_{dg} = V_g)$. This vector control allows independent decoupled control of the active and reactive power circulating between the grid and the converter which generate voltage references. Thus the grid side formulas are written as follows [26]

(18)
$$\begin{cases} V_{d\_f} = R_f i_{d\_f} + L_f \dfrac{di_{d\_f}}{dt} - \omega_g L_f i_{q\_g} + V_g \\ V_{q\_f} = R_f i_{q\_f} + L_f \dfrac{di_{q\_f}}{dt} + \omega_g L_f i_{d\_g} \end{cases}$$

where L_f and R_f are the filter inductance and resistance respectively, V_{d_f} and V_{q_f} are the converter d-axis and q-axis voltage components respectively, i_{d_f} and i_{q_f} are the d-axis current and q − axis current of Grid, V_g is the grid voltage components in the d-axis ,and ω_g is the network angular frequency. The powers exchanged through the filter to the network are expressed by

(19)
$$\begin{cases} P_g = V_{dg} i_{d\_f} + V_{qg} i_{q\_f} = V_g i_{d\_f} \\ Q_g = V_{qg} i_{d\_f} + V_{dg} i_{q\_f} = -V_g i_{q\_f} \end{cases}$$

So, the expressions for the direct and quadratic components of the current, respectively, are written as follows:

(20)
$$i_{d\_f}{}^* = \frac{P_g{}^*}{V_g}, i_{q\_f}{}^* = -\frac{Q_g{}^*}{V_g}$$

5.2. DC voltage control

The DC voltage is calculated using this equation [27]:

(21)
$$V_{DC} = \frac{1}{C}\int_0^\infty i_C dt$$

where i_C is the DC -bus current defined as

(22)
$$i_C = i_1 - i_2$$

where i_1 denote the stator's modulating current and i_2 denote the current provide to the network as shown in Fig. 7. The power transmitted to the grid is

(23)
$$P^* = V_{DC}\left(i_1 - i_2\right)$$

6. Simulation

The simulation is first run to demonstrate the suggested method's performance with the WRSG wind system's changeable wind speed and to compare the proposed AFLC-GAFOPI and GAFOPI controllers. Table 2. and 3. contain the parameters of WECS system. These control approaches are implemented using Matlab software. The simulation is made for two types of wind profiles.

Table 2. Parameters of the turbine, transformer and source [20]

Parameters	Units	Value
Rated power of the turbine, $P(t)$	Kw	10
Density area, ρ	$kg.m^{-2}$	1.225
Radius of the turbine, R	m	3
Number of blades	-	3
Viscous friction coefficient, F	$Nm.s.rad^{-1}$	0.017
Gear ratio, G	-	5.4
DC-Link voltage, V_{DC}	V	600
DC capacitance, C	μF	1500
Effective voltage, V_{rms}	V	220
Frequency, f	HZ	50
The leakage inductance, L_f	mH	12
Leakage resistance, R_f	Ω	1

6.1. Step-change

To analyze the controller's operation, a wind velocity profile as manner of a step change is given to the WTG model at first, as illustrated in Fig. 8(a). The wind speed began at 5.5m/s and abruptly increased to 7.5m/s, at time 1.5s. The wind speed is 9 m/s at time 3 s, and it has changed to 7 m/s at time 4 s. Figs. 8 illustrates the systems responses with the two controllers GAFOPI and AFLC-GAFOPI. In general, we can notice on the zooms of (Figs. (8b), (8c), (8d) and (8e)) that the performance of monitoring

variables of AFLC-GAFOPI controllers in comparison with GAFOPI controllers are less oscillating and have better time response characteristics and a fast stabilization, especially when a starting and at step change wind. Figs (8d) and (8f) we can also see that the overshoot has been reduced considerably.

Table 3. Parameters of the WRSG (LSA371, 4-poles)

Rated power of the generator, S_n	KVA	7.5
Stator resistance, r_s	Ω	1.19
Rotor resistance, r_f	Ω	3.01
Phase to phase rated voltage, U_{rms}	V	400
Direct synchronous reactance, X_d	pu	1.4
Transverse synchronous reactance, X_q	pu	0.7
Open circuit transient time constant, T_{d0}''	ms	522
Direct transient synchronous reactance, X_d'	pu	0.099
Direct sub transient synchronous reactance X_d''	pu	0.049
Direct transient time constant, T_d'	pu	40
Direct sub transient time constant, T_d''	ms	3.7
Armature time constant, T_a	ms	6
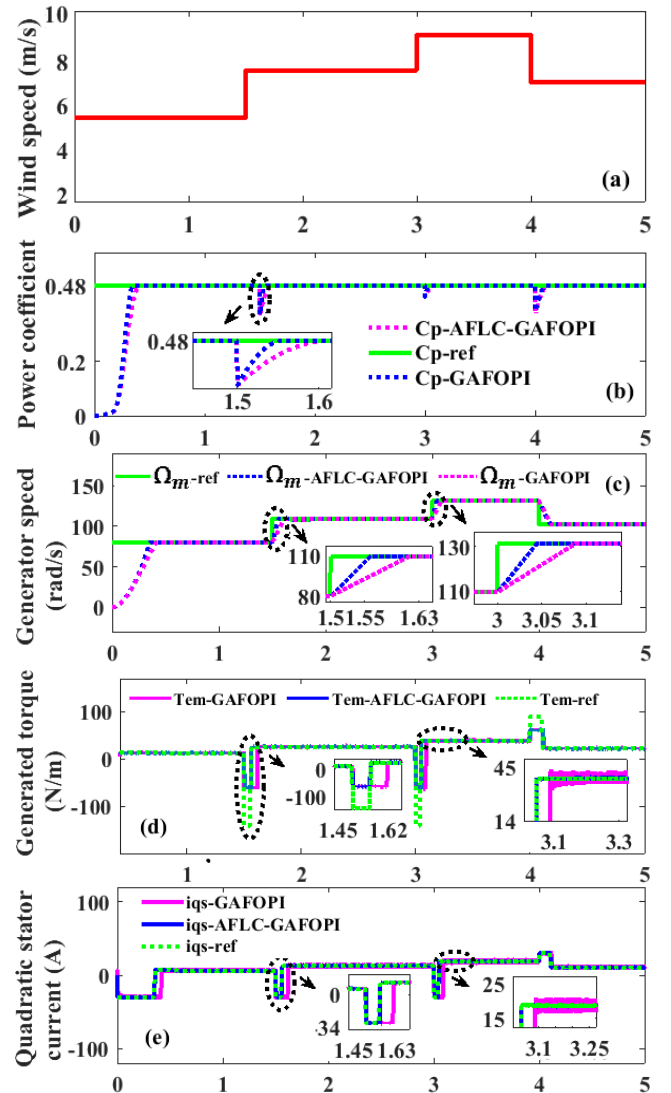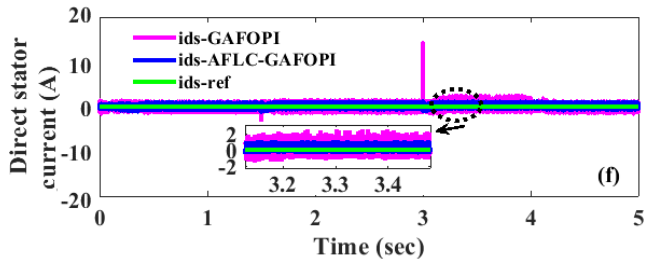
Fig. 8. Performance comparison under step-change wind of AFLC-GAFOPI and GAFOPI controllers. (a) wind speed profile, (b) Power coefficient, (c) Generator speed, (d) Generated torque, (e) Quadratic stator current, (f) Direct stator current.

6.2. Random wind

Similarly, we use the global wind chain model to apply a random wind profile see Fig. (9a) to assess how well the adaptive fuzzy logic controller-FOPI tracks and how efficient it is. The Fig. 9 represents the simulations results for the performances comparisons of the both controllers AFLC-GAFOPI and GAFOP for MSC side. Overall, we noted that all of the variables tracked the wind's evolution. Apart from the stator's direct current. The simulation results therefore show the excellence of the AFLC-GAFOPI controllers where the system responds and stabilizes quickly. Consequently, the simulation results reveal that oscillations in the system states were significantly decreased, demonstrating that AFLC-GAFOPI control methodology provides excellent dynamic performance in tracking system states under varying wind speeds and functions all right for WECS based on WRSG.
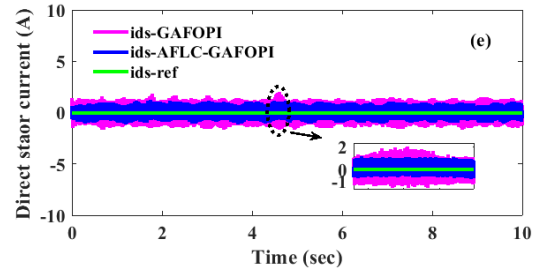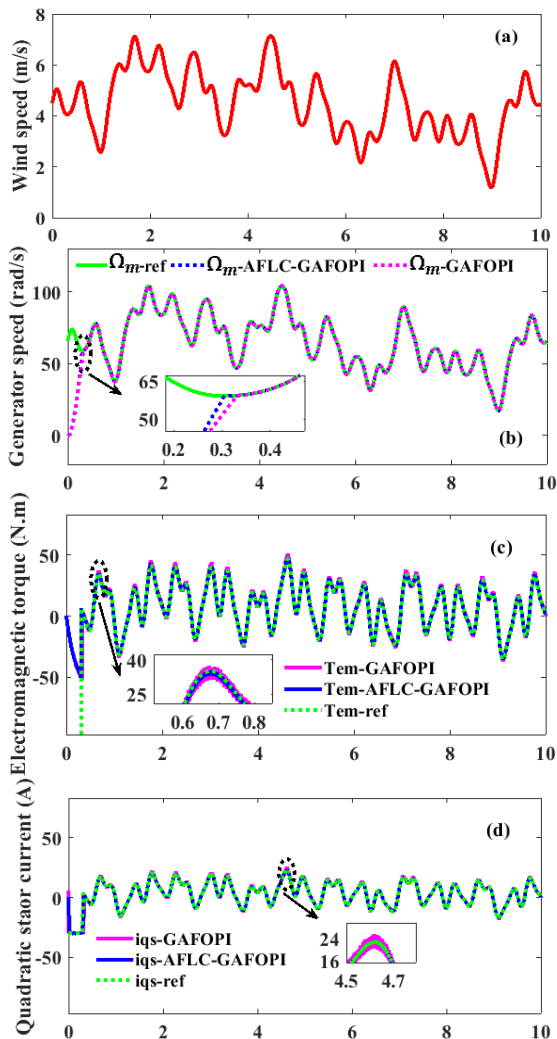
Fig. 9. Performance comparison under random wind speed for both controllers AFLC-GAFOPI and GAFOPI. (a) wind speed profile, (b) Power coefficient, (c) Generator speed, (d) Generated torque, (e) Quadratic stator current, (f) Direct stator current.
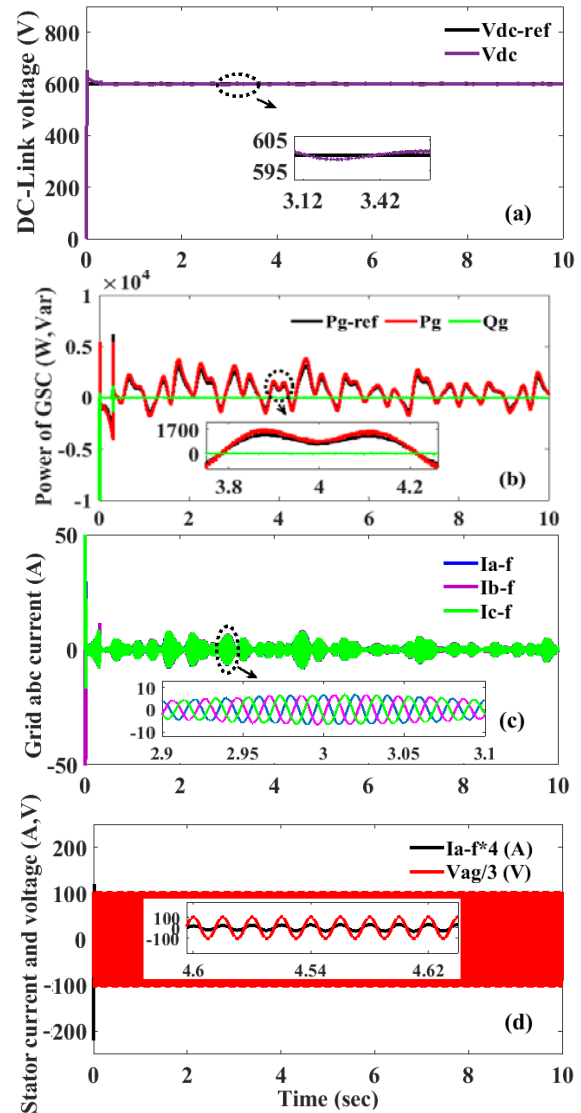
Fig. 10. Performance of the GSC under random wind speed using an AFLC-GAFOPI controller. (a) DC-link voltage, (b) active and reactive generator power, (c) grid abc currents, (d) zoom of grid current and voltage of phase a.

The intermediate circuit voltage is regulated to its reference of 600 V with a variation of roughly ±1 as illustrated in the simulation result for the GSC in Fig. (10a), the active and reactive power supplied into the grid are depicts in the Fig. (10b), the reactive power perfectly follows its reference Q_{ref} =0. While the active power is superimposed on its reference. The waveforms of the currents and their zooms with the voltage of phase a are

seen in Figs. (10c) and (10d) respectively, as can be observed, the grid current is nearly sinusoidal and the unit power factor of WECS is approximately reached.

7. **Conclusion**

In this article, the WRSG modeling and control method is described. In order to enhance the performance and robustness of the whole system against the intermittent nature of wind velocity and to reach MPPT of the WECS, a combination between two controllers GAFOPI and AFLC are designed. The GAFOPI is tuned using the GA algorithm, with the parameters optimized using the ITAE criterion, and the performance of the AFLC is determined by its MFs and rule base. The effectiveness of the proposed strategy AFLC-GAFOPI is then compared against GAFOPI in all wind velocity regimes, as shown by simulation results. In circumstances such as response rapidity, low error and overshoot as well as robustness under disturba GAFOPI controller.nces, the AFLC-GAFOPI controllers outperformed the

Authors: *Phd. Abdelkader Hafid Bouziane and Dr. Mohamed Debbat , University Mustapha Stambouli of Mascara, Algeria and Pr. Tahour Ahmed, School of Applied Sciences Tlemcen.*

E-mails : abdelkaderbouziane830@gmail.com
E-mails : mohamed.debbat@univ-mascara.dz
E-mails : tahourahmed@yahoo.fr

REFERENCES

[1] Biqnchi, F., Batista, H., Mantz, R. "Wind Turbine Control Systems: Principles, Modelling and Gain Scheduling Design", Springer- Verlag, London Limited; 2010.

[2] Belakehal, S., Benalla, H. and Bentounsi, A. " Power maximization control of small wind system using permanent magnet synchronous generator ". Revue des Energies Renouvelables, Vol. 12 N°2 307 – 319; 2009.

[3] Tahir, K., Belfedal, C., Alaoui, T., Champenois, G. "Power Control of Wind Turbine Based on Fuzzy Sliding-Mode Control" IJPEDS Vol. 5, No. 4, April 2015: 502 – 511.

[4] Gupta, A., Bhushan, H., Samuel, P. "Generator Topologies with Power Electronics Converters for a Wind Energy Conversion System", A Review.

[5] Kim, Y., Chung, Y., Moon, S. "Tuning of the PI Controller Parameters of a PMSG Wind Turbine to Improve Control Performance under Various Wind Speeds", Energies 2015, 8, 1406-1425.

[6] Zheng, W., Luo, Y., Chen, Y. and Wang, X. "A Simplified Fractional Order PID Controller's Optimal Tuning: A Case Study on a PMSM Speed Servo" 23, 130 Entropy 2021.

[7] Axtell, M., Bise, E. M. "Fractional Calculus Applications in Control Systems", Proceedings of the IEEE Nat. Aerospace and Electronics Conf., N.Y, pp 563-566, 1990.

[8] Chen, Y., Petras, I., Xue, D. "Fractional order control- a tutorial", In Proceedings of the American Control Conference (ACC'09), 1397–1411,2009.

[9] Podlubny, I. "Fractional-order systems and $PI^\lambda D^\mu$ controllers". IEEE Trans. On Automatic Control, vol.44, no. 1 pp. 208-213, 1999.

[10] Chen, L., Chen, G., Li, P., Lopes, A., "Machado J, Xu S. A variable-order fractional proportional-integral controller and its application to a permanent magnet synchronous motor", Volume 59, Issue 5, Pages 3247-3254, October 2020.

[11] Ying, H., William, S., James, J. "Fuzzy control theory: a nonlinear case", Automatica, 26(3) 513-520, (1990).

[12] Habibi, H., Yousefi koma, A., and Sharifian A. "power and velocity control of wind turbines by adaptive fuzzy controller during full load operation", Iranian Journal of Fuzzy Systems Vol. 13, No. 3, (2016) pp. 35-48.

[13] Yousaf, S., Mughees, A., Gufran khan, M., Ahmed amin, A., and Adnan, M. "A Comparative Analysis of Various Controller Techniques for Optimal Control of Smart Nano-Grid Using GA and PSO Algorithms", Digital Object Identifier 10.1109/ACCESS.2020.3038021.

[14] Dhaifallah, M., Kanagaraj, N., Nisar, K. "Fuzzy Fractional-Order PID Controller for Fractional Model of Pneumatic Pressure System", Hindawi Mathematical Problems in Engineering Volume 2018, Article ID 5478781, 9 pages.

[15] Khalfallah, T., Cheikh, B., Tayeb, A., Denai, M. and M'Hamed, D. "Robust and Efficient Control of Wind Generator Based on a Wound Field Synchronous Generator", Springer International Publishing AG 2018.

[16] Rekioua, D. "Wind Power Electric Systems", Modeling, Simulation and Control Springer-Verlag London, 2014.

[17] Xiong, L., Li, P., Ma, M.,Wang, Z., Wang, J. "Output power quality enhancement of PMSG with fractional order sliding mode control", volume 115, February 2020, 105402.

[18] Mouni, E., Tnani. S., Champenois, G. " Comparative study of three modelling methods of synchronous generator", in Conference of the IEEE Industrial Electronics Society, Paris, France, 2006.

[19] Errami, Y., Maaroufi, M., Ouassaid, M. "Control Scheme and Maximum Power Point Tracking of Variable Speed Wind Farm Based on the PMSG for Utility Network Connection", IEEE, 31.00/12/2-4766-4673-1-978, 2012.

[20] Tahir, K., Belfedal, C., Alaoui, T., Dena¨l, M., Doumi, M. "A new sliding mode stategy for variable-speed wind turbine power maximization", Int Trans Electr Energ Syst.e2513, 2018.

[21] Wang, H., Zeng, G., Dai, Y., Bi, D., Sun, J. and Xie, X. "Design of a Fractional Order Frequency PID Controller for an Islanded Microgrid: A Multi-Objective Extremal Optimization Method", Energies 2017, 10, 1502.

[22] Monje, C., Chen, Y., Vinagre, B., Xue, D., Feliu, V. "Fractional-order Systems and Controls Fundamentals and Applications" Springer, Verlag London Limited 2010.

[23] Wibowo, W., Jeong. S. "Genetic algorithm tuned PI controller on PMSM simplified vector control", J. Cent. South Univ, J. Cent. South Univ, 2013.

[24] Zheng, W., Pi, Y. "Study of the fractional order proportional integral controller for the permanent magnet synchronous motor based on the differential evolution algorithm", Volume 63, July 2016, Pages 387-393.

[25] Asri, A., Mihoub, Y., Hassaine, S., Logerais, P., Allaoui, T. "Intelligent maximum power tracking control of a PMSG wind energy conversion system", Asian J Control; 1–11, 2019.

[26] Mahersi, E., and Khedher, A. " Backstepping flux observer for nonlinear control of the direct-drive permanent magnet synchronous generator wind turbines", Wind Engineering, Vol. 40(6) 540–554, 2016.

[27] Mahersi, E., Kheder, A. "Adaptive backstepping Control applied to wind PMSG System", 978-1-4673-9768-1/16/31.00, IEEE 2016.